

Hanford Tank Farms Vadose Zone Monitoring Project

**Initial Calibration of the
Radionuclide Assessment System**

July 2001

Prepared for
U.S. Department of Energy
Grand Junction Office
Grand Junction, Colorado

Prepared by
MACTEC-ERS
Grand Junction Office
Grand Junction, Colorado

Approved for public release; distribution is unlimited.
Work performed under DOE Contract No. DE-AC13-96GJ87335.

Contents

	Page
Signature Page	iv
Abstract	v
1.0 Background	1
2.0 A Logging System for Waste Monitoring	2
3.0 Calibration Standards	6
4.0 System Dead Time Effect.....	7
5.0 Gain Drift and Measurement Precision.....	12
6.0 Calibration Measurements	16
7.0 Spectrum Stripping Methods	18
8.0 Preliminary Field Verification Acceptance Criteria	25
9.0 Acknowledgements	32
10.0 References	32

Tables

Table 1. Features of the Three RAS NaI (TI) Detectors	3
2. Preliminary RAS Window Settings	5
3. Calibration Standard Source Concentrations	7
4. Reference Standards for Calibration Source Concentrations	7
5. Data for the Calibration Measurement Sequence that Displayed the Largest Gain Shift	14
6. Data from Calibration Measurement that Showed Typical Gain Shift.....	15
7. Calibration Measurement Parameters	17
8. Calibration Count Rate Data	18
9. Full Spectrum Stripping Factors	20
10. Total Count Rate Stripping Demonstration	21
11. Filtered Spectrum Stripping Factors	21
12. Filtered Count Rate Stripping Demonstration	21
13. Spectrum Stripping Factors for the ¹³⁷ Cs Window	22
14. ¹³⁷ Cs Window Count Rate Stripping Demonstration.....	22
15. Spectrum Stripping Factors for the ⁶⁰ Co Window	23
16. Critical Values of <i>t</i> for the 95 and 99 Percent Confidence Intervals	27
17. Field Verifier Count Data for the RAS Small Detector.....	27
18. Count Acceptance Criteria for the RAS Small Detector.....	28
19. Count Rate Acceptance Criteria for the RAS Small Detector.....	28
20. Field Verifier Count Data for the RAS Medium Detector.....	29

Tables (continued)

Table 21. Count Acceptance Criteria for the RAS Medium Detector	29
22. Count Rate Acceptance Criteria for the RAS Medium Detector.....	29
23. Field Verifier Count Data for the RAS Large Detector.....	30
24. Count Acceptance Criteria for the RAS Large Detector.....	30
25. Count Rate Acceptance Criteria for the RAS Large Detector.....	31
26. Outcomes of Field Verification Measurements	31
27. Outcomes of Follow-Up Field Verification Measurements	32

Figures

Figure 1. NaI (TI) Spectrum from Standard SBM Compared to HPGe Spectrum	
From SBM	3
2. Total Count Rate Data Collected with the RAS Medium Detector for	
Investigation of Dead Time Effect.....	8
3. Filtered Count Rate Data Acquired With the RAS Medium Detector.....	10
4. An Extreme Example of Gain Shift	13
5. Examples of Parameter Changes Caused by Gain Shift.....	14

Hanford Tank Farms Vadose Zone Monitoring Project

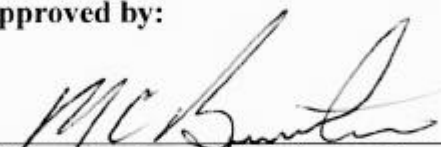
Prepared By:



Carl J. Koizumi, Technical Lead
MACTEC-ERS, Grand Junction Office


07-16-2001
Date

Approved by:



Michael Butherus, Task Order Manager
MACTEC-ERS, Grand Junction Office

7/16/01
Date



James F. Bertsch, Project Manager
MACTEC-ERS, Hanford

7/17/01
Date

Abstract

Hundreds of boreholes in the tank farms at the U.S. Department of Energy's (DOE) Hanford Site in Washington have been logged with high-purity germanium (HPGe) sensors. From the high-resolution spectra, gamma-ray-emitting radionuclides were identified and the in situ concentrations were determined, usually with accuracies comparable to laboratory sample assays.

Assayed radionuclides included fission fragments, neutron activation products, and processed uranium. These radionuclides, which will be referred to generically as "process wastes," were introduced to the subsurface by leaks in buried waste storage tanks, surface spills, and other inadvertent waste releases in the tank farms. The process wastes were produced by plutonium production and processing.

The next logical step is to periodically re-log subsurface zones within which contaminants may be migrating. The purpose of this monitoring will be to detect changes in radiation fields. Because the identities and concentrations of the radionuclides responsible for the radiation fields will not be a primary concern, high-resolution spectra will not be required. The monitoring logging system will be less complicated than the HPGe-based systems, and will acquire data using faster logging speeds and simpler operations.

A prototype logging system named the Radionuclide Assessment System (RAS) was designed to fulfill monitoring requirements. The RAS is equipped with three thallium-activated sodium iodide (NaI(Tl)) detectors that operate at the temperature of the environment. The low-resolution NaI(Tl) spectra will reveal changes in the subsurface radiation intensities, as desired, but will be useful to determine concentrations of gamma-ray-emitting radionuclides only under certain extremely favorable circumstances.

Because concentrations are not the objectives, the RAS has not been calibrated in the usual sense. That is, a correlation between instrument response and concentration has not been derived. Instead, certain characteristics of the system have been determined and are described in this report. For example, the system dead time effect was investigated and was found to be negligible, and measurement precision was determined to be adequate for monitoring.

On the basis of calibration spectra and spectra recorded with cesium-137 (^{137}Cs) and cobalt-60 (^{60}Co) sources, eight "windows" (groups of contiguous multichannel analyzer [MCA] channels) were established for data analysis. For example, a " ^{137}Cs window" extending from 570 to 740 kilo-electron volts (keV) will tally counts due to the 661.6-keV gamma ray of ^{137}Cs . The ^{137}Cs window, and the other windows, will also collect background counts; therefore, a method to subtract natural background counts from various windows was derived so that concentration calculations can be done if it is eventually found feasible to correlate window counts to concentrations.

A portable, sealed potassium-uranium-thorium source was acquired for measurements in the field to verify the performance of the logging system. Using this source, about a dozen spectra have been

acquired with each NaI(Tl) detector. Analyses of these spectra yielded preliminary “field verification criteria.” During logging operations, new field verification spectra will be periodically recorded, and analyzed results will be compared with the field verification criteria to confirm that the logging system is operating properly.

1.0 Background

At nuclear reactors and plutonium processing facilities at the Hanford Site, plutonium for the national defense was produced and processed for more than forty years following World War II. Much of the high-level radioactive waste from these activities has been stored for decades in large underground tanks. Approximately 67 of the 149 tanks of the “single shell” design have leaked high-level waste into the thick layers of unsaturated sediments (vadose zone) surrounding the tanks.

Over the years, hundreds of boreholes have been drilled around the waste storage tanks. In the 1960s, a leak detection activity was instituted to monitor for tank leaks by logging the boreholes with passive gamma-ray sensors (Isaacson 1982). The gross count data could not be used to identify gamma-ray-emitting nuclides or determine their concentrations, but these factors were unimportant because all that was needed for leak detection was an ability to detect gamma-ray anomalies. When the plutonium processing was ongoing, the fresh waste could be readily detected because of intense gamma-ray intensities resulting from abundances of short-lived ruthenium-106 (^{106}Ru , half life = 368 days).

During years of operations, waste spills and pipeline leaks added to the contamination in the vadose zone. Meanwhile, most of the ^{106}Ru has decayed to undetectable levels, but longer lived radionuclides, such as cesium-137 (^{137}Cs) and cobalt-60 (^{60}Co), remain. A decision to characterize the gamma-ray-emitting contaminants in the vadose zone at all the single-shell tank (SST) groups (tank farms) on the Hanford Site was made by the DOE Richland Operations Office (DOE-RL) in 1994. DOE-RL assigned the characterization work to the DOE Grand Junction Office (DOE-GJO) in Grand Junction, Colorado, a site with an extensive set of borehole calibration standards and experience in borehole radiation measurements. In 1999 the DOE Office of River Protection (DOE-ORP) was created and the Hanford tank farms are presently the responsibility of that organization.

DOE-GJO began the waste characterization logging in 1995 with two spectral gamma-ray logging systems (SGLSs) that were designed specifically for that project. Each of these units has a sonde with a p-type coaxial 35-percent-efficient HPGe detector. Through analyses of full energy peaks in the high-resolution passive gamma-ray spectra, various gamma-ray emitters, which included ^{137}Cs , ^{60}Co , europium-152 (^{152}Eu), europium-154 (^{154}Eu), uranium-235 (^{235}U), uranium-238 (^{238}U), and others, were identified and profiles of radionuclide concentrations in relation to depth were compiled.

Logging soon revealed zones with gamma-ray intensities higher than the level (corresponding to about 10^4 picocuries¹ per gram [pCi/g] of ^{137}Cs) at which the SGLS detectors become unable to record spectra with full energy peaks. Determination of the contaminant distributions in such zones required an instrument of lower efficiency, and in 1999 DOE-GJO deployed a high rate logging system (HRLS). The HRLS sonde has a planar 6-millimeter by 8-millimeter n-type HPGe detector that is able, with two auxiliary shields installed, to acquire useful gamma-ray spectra in gamma-ray intensities corresponding to 10^8 pCi/g of ^{137}Cs .

¹ A picocurie is 10^{-12} of a curie; a curie is defined as 3.7×10^{10} decays per second.

The baseline characterization was completed in 2000. Essentially all of the approximately 800 existing Hanford tank farm boreholes were logged with SGLSs, and zones of extreme gamma activity were re-logged with the HRLS. The results of the baseline characterization are described in documents posted at Internet address <http://www.gjo.doe.gov/programs/hanf/HTFVZ.html>.

2.0 A Logging System for Waste Monitoring

The baseline characterization results have been examined, along with historical gross count data, to identify subsurface zones that show evidence of contaminant migration. Boreholes that penetrate such zones will be relogged periodically to interrogate for changes in radionuclide distributions.

The SGLSs are not well suited to repetitive logging of the boreholes, mainly because of slow logging speeds and cryogenic detector operating requirements. Logging to monitor for changes in radionuclide distributions or concentrations should be performed with a unit capable of faster logging speeds and simpler operations. A prototype unit, the Radionuclide Assessment System (RAS), was designed and fabricated by DOE-GJO to meet these requirements. The RAS is a mobile, self-contained logging system that will acquire low-resolution passive gamma-ray spectra. The RAS sonde has an upper section containing a multichannel analyzer and the telemetry components. Any one of three modules can be connected to this section. Each module has a NaI(Tl) crystal and photomultiplier. Table 1 shows dimensions and other features of the three detector crystals.

Table 1. Features of the Three RAS NaI(Tl) Detectors

Informal Name	Crystal Diameter and Length (inches)	Intended Use
Small Detector	1.0 by 1.0	This low-efficiency detector is designed to acquire passive gamma-ray spectra in intense radiation fields. Radiation is collimated by 1-inch-thick lead shields above and below the crystal.
Medium Detector	1.5 by 2.0	This medium-efficiency detector is designed to acquire passive gamma-ray spectra in moderate radiation fields. There is no lead shielding around this crystal.
Large Detector	3.0 by 12.0	This high-efficiency detector is designed to acquire passive gamma-ray spectra in low radiation fields. There is no lead shielding around this crystal.

All of the RAS detectors are capable of recording spectra with full energy peaks, but the energy resolution of any peak will be much poorer than the corresponding peak resolution for an SGLS spectrum. The two spectra in Figure 1 provide a comparison of NaI(Tl) resolution and HPGe resolution. The source for both spectra was a calibration standard named SBM that contains a mixture of natural ^{40}K , ^{238}U , and ^{232}Th (see Table 3). The spectrum labeled “NaI(Tl)” is spectrum MMSAN003.CHN from the 2000 RAS medium detector calibration measurements. The spectrum labeled “HPGe” is spectrum SBMC5004.CHN from the 1999 SGLS Gamma 2B calibration measurements.

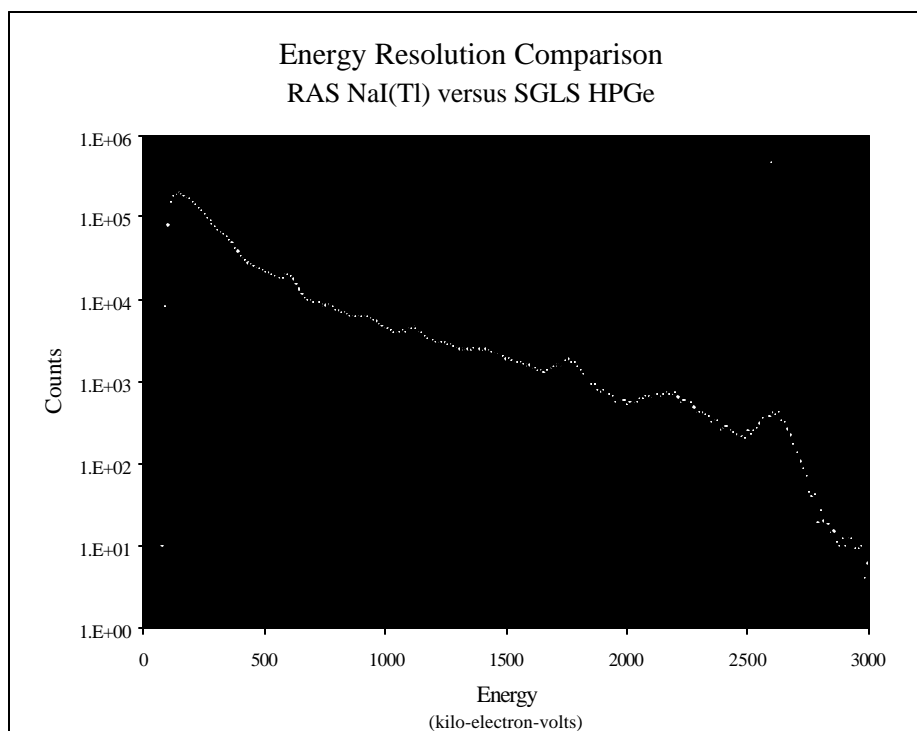


Figure 1. NaI(Tl) Spectrum from Standard SBM Compared to HPGe Spectrum from SBM

Most of the “peaks” in the NaI(Tl) spectrum in Figure 1 overlap several peaks in the HPGe spectrum, indicating that a RAS spectral peak can often contain responses from several gamma rays with similar energies. Multiple gamma-ray sources commonly occur in the Hanford subsurface; therefore, peaks in corresponding RAS spectra are likely to contain contributions from several gamma-ray sources. Consequently, there will usually be no way to correlate the intensities of such peaks to the concentrations of gamma-ray emitters. However, concentrations are not objectives of RAS data analysis. Instead, RAS data will be analyzed to assess changes in concentrations or distributions of gamma-ray emitters.

RAS spectra will be analyzed by total counts and/or window² counts. The initial window analyses will utilize eight spectral windows. Preliminary settings for these windows are displayed in Table 2. The energy ranges were determined through reviews of window settings established for measurements supporting the National Uranium Resource Evaluation (NURE³) program (Wilson and Stromswold 1981), and through analyses of spectra acquired during performance testing of the RAS at DOE-GJO in 1996. The corresponding MCA channel number settings were determined from spectra collected in March 2001 using an Amersham K-U-Th field verification source (Amersham part name: *KUTh Field Verifier*; part number: 188074). The small and medium detectors had the same settings in channel numbers (Table 2), while the settings for the large detector were slightly different. The window settings may be changed after experience with the spectra is gained.

² A window is a section of a spectrum defined by a contiguous group of MCA channels. Although the lower and upper window boundaries are set by MCA channel numbers, the levels are usually specified in kilo-electron-volts.

³ NURE was conducted by DOE-GJO from 1974 to 1984 to assess the uranium resources of the United States. The project supported significant research and development in nuclear logging. The borehole calibration standards that are now used to calibrate radiation sensors for environmental surveys were designed and constructed under the NURE.

Table 2. Preliminary RAS Window Settings

Name of Window	Range (keV)	Approximate Range (MCA Channels)			Source and Energy of Target Gamma Ray
		Small Detector	Medium Detector	Large Detector	
Lithology ¹	0 – 570	0 – 51	0 – 51	0 – 50	None
¹³⁷ Cs	570 – 740	52 – 66	52 – 66	51 – 64	¹³⁷ Cs (661.6 keV)
Mid-Range ²	740 – 940	67 – 83	67 – 83	65 – 82	None
^{234m} Pa	940 – 1060	84 – 93	84 – 93	83 – 92	^{234m} Pa ³ (1001.0 keV)
⁶⁰ Co	1060 – 1390	94 – 121	94 – 121	93 – 121	⁶⁰ Co (1173.2 keV, 1332.5 keV)
⁴⁰ K	1390 – 1600	122 – 138	122 – 138	122 – 139	⁴⁰ K (1460.8 keV)
²³⁸ U	1600 – 2400	139 – 202	139 – 202	140 – 209	²¹⁴ Bi ⁴ (1764.5 keV, 2204.1 keV)
²³² Th	2400 – 2800	203 – 255	203 – 255	210 – 255	²⁰⁸ Tl ⁵ (2614.5 keV)

¹ The counts in this window will be influenced by the “Z effect.” See Section 4.0, “System Dead Time Effect.”

² This window occupies the gap between the ¹³⁷Cs and ^{234m}Pa windows. It has no use at present.

³ ^{234m}Pa is the third nuclide in the uranium decay series. ^{234m}Pa and the nuclide that precedes it in the uranium decay series, ²³⁴Th, have such short half lives (1.2 minutes and 24 days, respectively) that the existence of ^{234m}Pa essentially guarantees that ²³⁸U is also present. Spectral peaks for the ^{234m}Pa gamma rays are rarely observed in association with natural uranium because the gamma-ray yields are so low, but a high concentration of processed ²³⁸U will be revealed by a prominent peak due to the 1001.0-keV ^{234m}Pa gamma ray.

⁴ Bismuth-214 (²¹⁴Bi) is the tenth nuclide in the uranium decay series. Because a long-lived nuclide (radium-226, half life = 1620 years) and an inert gas (radon-222) occur between ²³⁸U and ²¹⁴Bi in the uranium decay series, the existence of ²¹⁴Bi does not necessarily imply that ²³⁸U is also present. Nonetheless, the 609.3-, 1764.5-, and 2204.1-keV ²¹⁴Bi gamma rays have high yields and are often used to assay naturally occurring ²³⁸U.

⁵ Thallium-208 (²⁰⁸Tl) is the tenth nuclide in the thorium decay series.

Windows were designated for ¹³⁷Cs and ⁶⁰Co because they are by far the most widespread process waste components detected by the baseline survey, and when they occur unmixed with other radionuclides, the window count rates might be related to the concentrations.

Processed uranium (mixture of ²³⁵U and ²³⁸U) was also detected fairly frequently. The ^{234m}Pa window is intended to tally counts associated with the 1001.0-keV ^{234m}Pa gamma ray.

The ⁴⁰K, ²³⁸U, and ²³²Th windows will acquire counts due to naturally occurring potassium, uranium, and thorium. Count rates in these windows may be useful for detection of lithology changes and determination of backgrounds in the ¹³⁷Cs, ⁶⁰Co, and ^{234m}Pa windows.

¹⁵²Eu and ¹⁵⁴Eu were also detected during the baseline work. Principal gamma rays associated with these nuclides have the following energies: 121.8, 344.3, 778.9, 964.0, 1085.8, 1112.1, and 1408.1 keV (¹⁵²Eu); 123.1, 723.3, 873.2, 996.3, 1004.8, and 1274.8 keV (¹⁵⁴Eu). The higher energy ¹⁵²Eu and ¹⁵⁴Eu gamma rays will contribute counts to the ¹³⁷Cs and/or ⁶⁰Co windows, as will the 1001.0-keV gamma ray of ^{234m}Pa. Thus, when process waste is present, the two windows can have elevated count

rates even if ^{137}Cs and ^{60}Co are absent. The ^{137}Cs and ^{60}Co windows therefore serve as indexes for the process wastes. Elevated window count rates will indicate the presence of process waste, and changes in those count rates over time will imply that the concentrations of process waste constituents are changing. It will not be necessary to identify the source radionuclides to infer changes in concentrations.

The ^{137}Cs and ^{60}Co windows will also acquire full energy peak counts as well as Compton continuum contributions for the gamma rays emitted by the naturally occurring gamma-ray emitters. However, the concentrations of ^{40}K , ^{238}U , and ^{232}Th at any point in the subsurface are expected to be constant over time; thus, the natural emitters will not influence the monitoring for changes in the ^{137}Cs and ^{60}Co window counts.

3.0 Calibration Standards

The Hanford Site has a calibration center for borehole radiation sensors near the Meteorology Station, north of the main entrance to the 200 West Area. The calibration standards and their links to New-Brunswick-Laboratory-certified standards, and other standards, are described in Heistand et al. (1984) and Steele and George (1986). These references refer to the Hanford facilities as the “Spokane SBL/SBH, SBT/SBK, SBU/SBM, and SBA/SBB Models.” The “Spokane” designation refers to the original installation of these standards by DOE-GJO in the early 1980s at a calibration center near Spokane, Washington, for the calibration of borehole sensors. In 1989, the Spokane standards were moved to DOE’s Hanford Site.

Each model has two radiation standards with elevated concentrations of ^{40}K , ^{238}U , or ^{232}Th . The radiation sources are indicated by the model names. For example, the SBT/SBK Model has a thorium-rich standard, SBT $\underline{\text{T}}$, and a potassium-rich standard, SBK $\underline{\text{K}}$. “S” and “B” stand for Spokane and Borehole. The source “concentrations” (actually, decay rates per unit mass) are shown in Table 3.

Table 3. Calibration Standard Source Concentrations

Standard	Main Design Application	⁴⁰ K Concentration (pCi/g)	²²⁶ Ra Concentration ¹ (pCi/g)	²³² Th Concentration (pCi/g)
SBK	elevated K spectral standard	53.50 ± 1.67	1.16 ± 0.11	0.11 ± 0.02
SBT	elevated Th spectral standard	10.63 ± 1.34	10.02 ± 0.48	58.11 ± 1.44
SBA	low U fission neutron standard	undetermined	61.2 ± 1.7	undetermined
SBM	mixed K, U, Th spectral standard	41.78 ± 1.84	125.79 ± 4.00	39.12 ± 1.07
SBU	elevated U spectral standard	10.72 ± 0.84	190.52 ± 5.81	0.66 ± 0.06
SBL	low U total count standard	undetermined	324 ± 9	undetermined
SBB	high U fission neutron standard	undetermined	902 ± 27	undetermined
SBH	high U total count standard	undetermined	3126 ± 180	undetermined

¹ These standards contain uranium minerals in which radium-226 (²²⁶Ra) is essentially in decay equilibrium with ²³⁸U. Consequently, in each standard the concentration of ²³⁸U can be considered equal to the concentration of ²²⁶Ra (when the concentrations are expressed in terms of decay rate per unit mass).

Table 4 lists the gamma-ray counting standards to which the source concentrations in the borehole standards are referenced.

Table 4. Reference Standards for Calibration Source Concentrations

Source	Reference Standard
Potassium (⁴⁰ K)	reagent-grade potassium carbonate (K ₂ CO ₃)
Radium (²²⁶ Ra)	NBL (New Brunswick Laboratory) 100-A Series Uranium ¹
Thorium (²³² Th)	NBL 100-A Series Thorium ¹

¹ Trahey et al. (1982).

The various mixtures of ⁴⁰K, ²²⁶Ra (uranium), and ²³²Th, along with the large range of radium (uranium) concentrations, provided the gamma-ray signals needed to accomplish the measurement goals, which were assessment of the system dead time effect, evaluation of measurement precision, and development of several spectrum stripping methods.

4.0 System Dead Time Effect

During performance testing of the RAS at DOE-GJO in 1996, spectra were acquired by logging the following standards (Leino et al. 1994) with the small, medium, and large detectors:

U Model, ^{226}Ra (^{238}U) concentration = 162.9 ± 5.3 pCi/g
 N-3 Model, ^{226}Ra (^{238}U) concentration = 654 ± 23 pCi/g
 U-3 Model, ^{226}Ra (^{238}U) concentration = 1278 ± 51 pCi/g
 U-2 Model, ^{226}Ra (^{238}U) concentration = 3478 ± 218 pCi/g
 U-1 Model, ^{226}Ra (^{238}U) concentration = 7459 ± 465 pCi/g.

Conclusions about system dead time were drawn from the performance test data and data acquired by logging the Hanford standards listed in Table 3. No casings were placed in the standards during dead time data acquisition. Data were analyzed to investigate dead time effects and the source self-absorption effect, or “Z effect” (Z is the average atomic number of the calibration standard material). The dead time effects were determined to be negligible, but the Z effect was not negligible. The rest of this section describes the measurements and analyses that support this conclusion.

Total count rate data acquired with all three detectors showed similar trends in relation to ^{238}U concentration. The trends are illustrated by data collected with the medium detector. For this detector, the system dead time ranged from about 6 percent (U Model) to approximately 63 percent (U-1 Model). A plot of the average total count rate in relation to the ^{238}U concentration is depicted by triangular data points (labeled “Uncorrected”) in Figure 2.

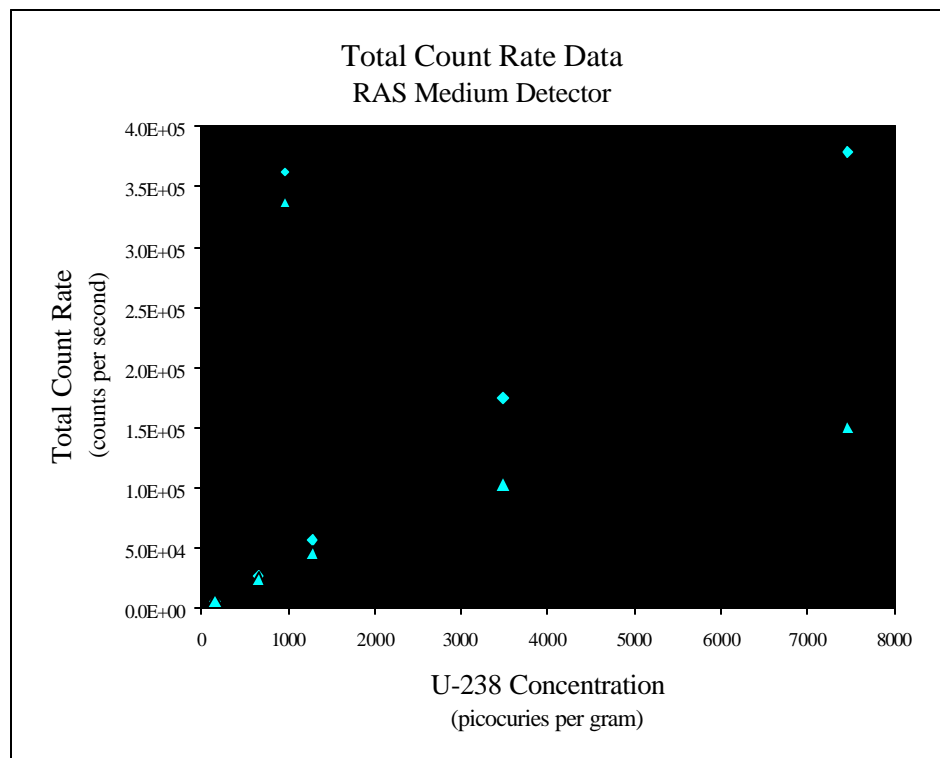


Figure 2. Total Count Rate Data Collected with the RAS Medium Detector for Investigation of Dead Time Effect

The (triangular) points for the higher total count rates depart from a linear relationship in a way that could be easily mistaken for a dead time effect. In fact, during the NURE program, DOE-GJO

proposed the use of such data to determine the value of the dead time constant, t , that is characteristic of a nonparalyzable logging system. The constant t is a factor in a well known equation that expresses the dead-time-corrected count rate n in terms of the recorded count rate m (Knoll 2000):

$$n = \frac{m}{1 - m \cdot t}. \quad \text{Eq. (1)}$$

During NURE, values of t were calculated with a DOE-GJO computer program named “MULTIPIT” (Crew 1979). Total count rates (m) would be recorded by logging three or more of the GJO standards with high ^{238}U concentrations. With these count rates and an assumed value for t , MULTIPIT would use Equation (1) to calculate the n values, then would check the relationship between the n values and the ^{238}U concentrations. If the relationship was nonlinear, the program would change the t value, recalculate the n values, and check the relationship again. This iterative procedure continued until the relationship between the n values and the ^{238}U concentrations was as close to linear as achievable. The associated value for t was then assigned to the logging system as the dead time constant, and was used thereafter to “correct” log data.

If applied to the RAS medium detector data, the MULTIPIT procedure produces a value $t = 4$ microseconds. With this t value and the recorded total count rates, Equation (1) gives the “corrected” total count rates that are represented in Figure 2 as diamond-shaped points.

Although this analysis superficially resembles a normal dead time determination, the MULTIPIT method actually does not yield a dead time correction because of a critical difference between the calibration standard measurements and conventional dead time measurements. For conventional dead time measurements, several point gamma-ray sources are placed in the vicinity of the detector, with only air occupying the spaces between sources and detector. In contrast, a borehole or calibration standard measurement has the *gamma-ray sources embedded in a mass of dense material* which surrounds the sonde. When the sources are distributed within material, emitted radiation is susceptible to interactions within that material. In the interaction responsible for the Z effect, photoelectric absorption, photons disappear. Because the photoelectric interaction cross section is inversely related to the photon energy and directly related to Z , the probability of absorption within the medium is high if the photon energy is low, and a higher fraction of photons is absorbed in a medium of high Z than in a low- Z medium.

The dependence of the photoelectric effect on Z is important because the calibration standards contain varying concentrations of uranium, and uranium has the highest atomic number ($Z = 92$) of the naturally occurring elements. Although gamma rays from uranium and its decay progenies are created within a standard at a rate proportional to the uranium concentration, the count rate recorded by logging the standard will not necessarily be similarly proportional to the uranium concentration because a Z -dependent fraction of the photon flux will be suppressed by photoelectric absorption. The rise in photoelectric absorption that accompanies an increase in Z leads to a nonlinear relationship between total count rate and uranium concentration, such as shown in the plot represented by triangular points in Figure 2.

Wilson and Stromswold (1981) studied the effects on gamma-ray logs of photoelectric absorption within media that had anomalous Z values caused specifically by elevated concentrations of uranium. Wilson and Stromswold (1981) concluded that the Z effect hardly perturbs the part of a spectrum above about 500 keV if the uranium concentration is lower than 0.6 percent uranium (2,000 pCi ^{238}U per gram). Typically, however, most of the counts in a spectrum occur in the part below 500 keV; therefore, the Z effect can influence the total count, even if the uranium concentration is lower than 0.6 percent.

If the Z effect primarily influences the portion of a spectrum below 500 keV, then the effect can be greatly reduced by tallying counts in only those MCA channels that correspond to energies higher than 500 keV. For the RAS measurements, a setting of 570 keV was chosen and the 1996 spectra were re-analyzed by manually controlling the spectrum analysis program to tally only counts corresponding to photon energies above 570 keV. In essence, this “filtering” yielded the same results that would have been recorded if a lower level discriminator had been electronically imposed at 570 keV.

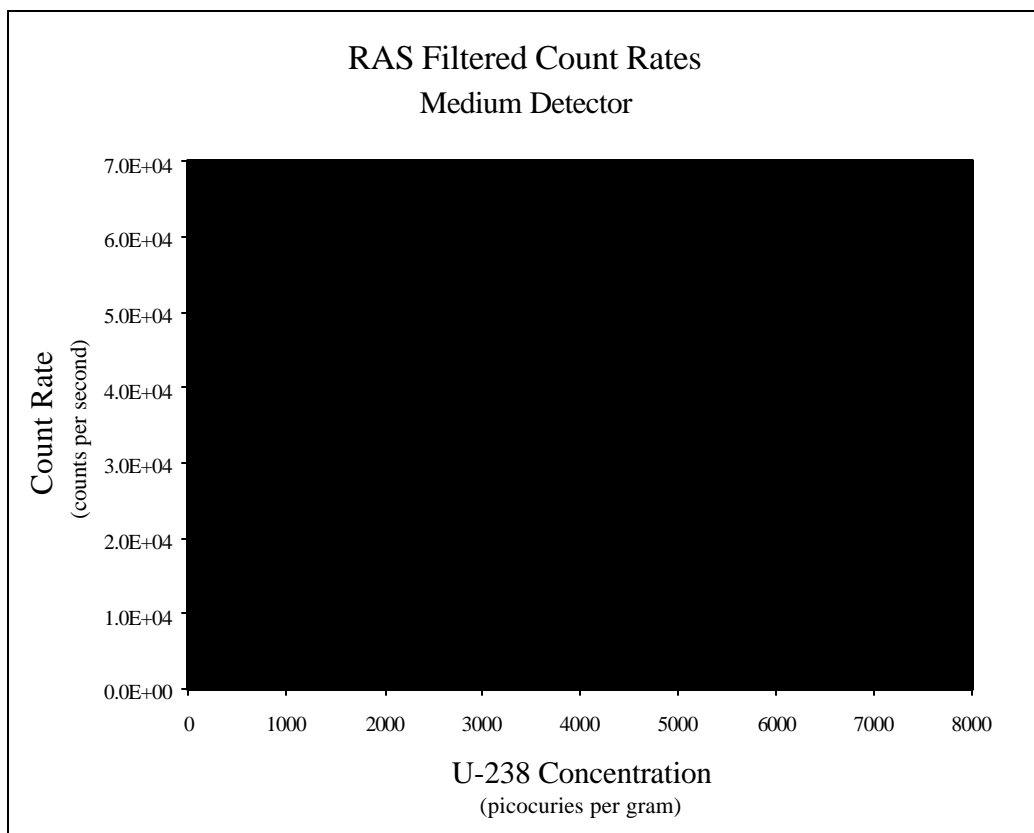


Figure 3. Filtered Count Rate Data Acquired with the RAS Medium Detector

Diamond-shaped points in Figure 3 depict the filtered count rates plotted in relation to ^{238}U concentration. Data collected in 2000 by logging the Hanford calibration standards SBU, SBL, SBB, and SBH (see Table 3) were analyzed similarly, and points representing those measurements are depicted by triangles in Figure 3. All of the points, diamonds and triangles, lie along the same curve,

which is close to a straight line. Points for the SBH, U-2, and U-1 standards fall approximately along the line, even though those standards have ^{238}U concentrations exceeding the Wilson-Stromswold upper limit of 2,000 pCi/g.

The nearly linear trend of the data points in Figure 3 indicates that the nonlinearity displayed by the triangular points in Figure 2 was caused entirely by the Z effect. It follows that the dead time effect must be negligible, at least for dead times up to the highest achieved in the measurements, which was about 63 percent for the medium detector.

Analyses of filtered and unfiltered data for the small and large detectors led to similar conclusions. The system dead time effect is small, but the Z effect is significant. The data indicate that the dead time effect is negligible for dead times up to 35 percent for the small detector, and up to 69 percent for the large detector.

Equation (1) should not be viewed as a way to correct for the Z effect. Although the equation, with $t = 4$ microseconds, did produce “corrected” medium detector count rates that were linear in relation to source intensity, the “correction” is applicable only if the Z effect is caused by uranium. If applied, for example, to a high count rate due to ^{137}Cs , Equation (1) would yield an overcorrected rate because ^{137}Cs has a much smaller atomic number than ^{238}U (55 versus 92), and the fraction of photons absorbed within the ^{137}Cs -contaminated medium would be much less than if the medium had a high concentration of uranium.

Because filtering negates the Z effect, it might seem worthwhile to filter spectra routinely. However, filtering removes a large fraction of the counts in a spectrum. For example, for the medium detector, the average total count rate for the DOE-GJO U-3 standard was 46.5×10^3 counts per second, while the average filtered count rate was only 7.5×10^3 counts per second. Because the relative statistical uncertainty increases as the number of counts decreases, filtering increases the relative count uncertainty.

This argues against filtering as a routine part of data analysis, especially in the early part of the monitoring program, when no attempts will be made to derive source concentrations from the monitoring data. In the beginning of the program, statistically significant changes in the total count rate or selected window count rates will be used as indicators of changes in process waste concentrations.

Filtering will probably be unnecessary in general anyway because most of the contaminated zones at Hanford will not have extreme Z values. ^{238}U is not the most common waste constituent at Hanford; the most abundant by far is ^{137}Cs . Because the atomic number of ^{137}Cs is much smaller than the atomic number of ^{238}U , the ^{137}Cs atom density must far exceed the ^{238}U atom density to produce a given Z anomaly. ^{137}Cs also has a much shorter half life than ^{238}U (30.2 years versus 4.5×10^9 years). Thus, the activity per unit volume of ^{137}Cs corresponding to the Z effect threshold is far higher than the 2×10^3 pCi/g that Wilson and Stromswold (1981) identified as the ^{238}U threshold. For ^{137}Cs , the threshold is around 5×10^{11} pCi/g, and concentrations this high have not been encountered by logging at Hanford.

The fact that the 2000 data from the standards SBU, SBL, SBB, and SBH followed the same trend set by the 1996 data indicates that the properties of the logging system, such as the efficiency, have not

changed since the performance tests were done in 1996; therefore, it was valid to combine the 1996 and 2000 data for the dead time study.

The remarks on Z effect and filtering apply to total count or total count rate data. Future experience at Hanford may eventually show that some source concentrations can be derived from RAS window count rates. The lowest-energy window with this potential will be the ^{137}Cs window, which spans the energy range from 570 to 740 keV. This energy range is high enough so that counts in this window will not be seriously influenced by the Z effect.

5.0 Gain Drift and Measurement Precision

Before calibration measurements commenced, experiments to assess the RAS gain stability were performed. Because temperature change is a principal cause of gain shift, the performances of the three detectors were monitored under temperature fluctuations using a fixture fabricated by GTS Duratek (a DOE Hanford Site contractor). The sonde to be tested was placed inside of a 5-foot long section of 8-inch-diameter steel casing that is spiral wrapped with plastic tubing. Water at various temperatures was circulated through the plastic tubing while temperatures were monitored with thermocouples attached to the casing and tool housing. ^{137}Cs and ^{60}Co button sources were used as gamma-ray sources.

These tests were inconclusive because minor gain shifts accompanied temperature changes, but large gain shifts occurred when the sonde was inserted into or withdrawn from the casing fixture. This indicated that magnetic effects on the photomultiplier are a major cause of gain shifts. The hypothesis receives further support from field tests that showed that the gain is significantly perturbed by casing welds. The degree to which the sensitivity to magnetic fields affects spectral data is unknown at present, but the magnetic effects are a clear cause for concern. To mitigate the effects, mu-metal shields have been retrofitted on the photomultiplier tubes of the small and medium detectors. (The spacing around the large detector photomultiplier tube was too small for shielding.)

Gain shifts sometimes occur for unknown reasons when the temperature of the sonde is stable and there is no casing or other ferromagnetic material near the sonde. The two spectra depicted in Figure 4 show the most extreme example of gain shift observed in the calibration data. The two spectra were recorded in January 2001 by logging the Hanford SBT standard with the medium detector. The spectrum (named MTUA8000.S0) with the arrow pointing to the

2614.5-keV gamma-ray peak was recorded at the beginning of the calibration measurement sequence; the other spectrum (named MTUA8005.S0) was recorded at the end of the sequence. During the measurement sequence the sonde was held stationary and the temperature in the test hole remained nearly constant, yet a significant gain shift occurred over the 1.4-hour data acquisition period. The offset is largest at the high-energy end; the center of the 2614.5-keV gamma-ray peak shifted from channel 217 to channel 210. Offset is nearly nonexistent at the low-energy end because gain shift “stretches” or “compresses” a spectrum as if the low-energy end were fixed. The largest gain shift

effects were imposed on the high-energy window count rates, while the total count rates were not as seriously affected. This is illustrated by the window and total count rates compiled in Table 5.

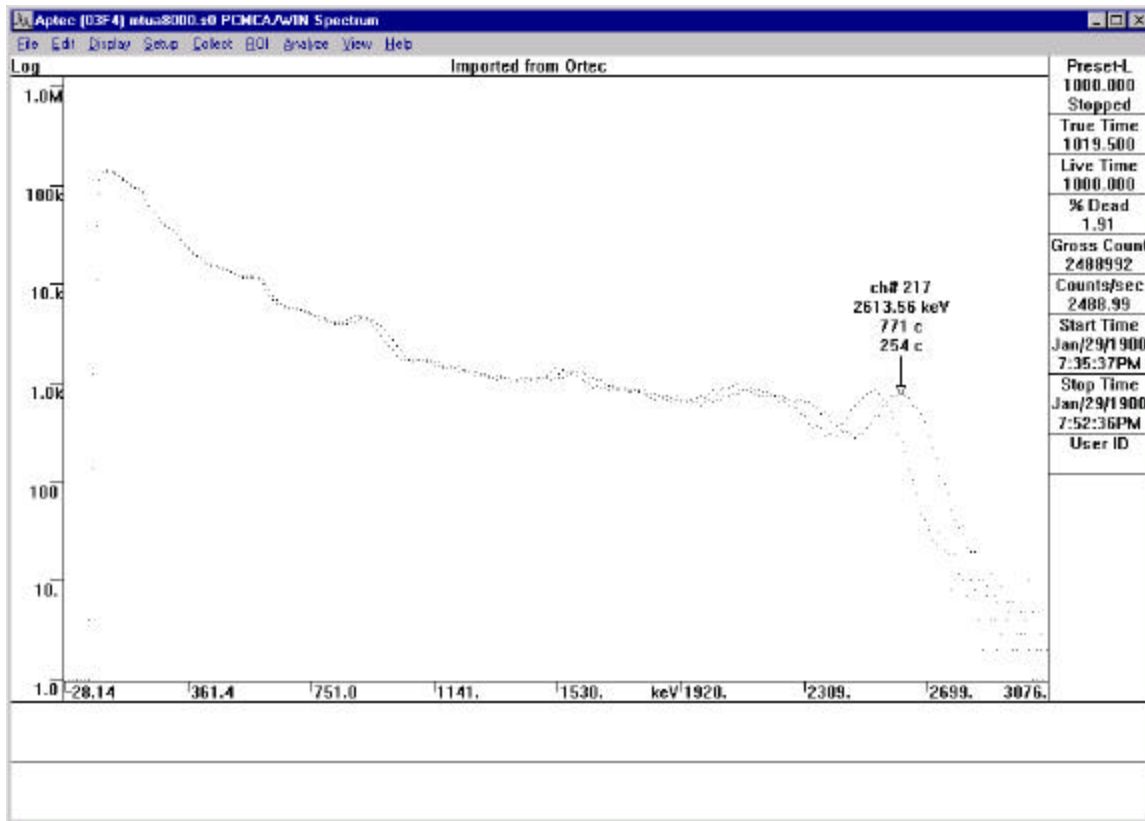


Figure 4. An Extreme Example of Gain Shift. (The start and stop dates are incorrect because the analysis software was not Y2K-compliant.)

Table 5. Data for the Calibration Measurement Sequence that Displayed the Largest Gain Shift.
The last row in the table shows the net percent change for each parameter.

Spectrum Name	¹³⁷ Cs Window (Channels 50-64) Count Rates (c/s)	²³⁸ U Window (Channels 136-200) Count Rates (c/s)	²³² Th Window (Channels 201-255) Count Rates (c/s)	Total (Channels 0-255) Count Rates (c/s)	Center of 2614.5-keV Gamma-Ray Peak (Channel Number)
MTUA8000.S0	94.43 ± 0.61	46.53 ± 0.43	12.28 ± 0.22	2489.0 ± 3.2	216.2
MTUA8001.S0	91.72 ± 0.61	45.70 ± 0.43	11.51 ± 0.21	2470.6 ± 3.1	214.3
MTUA8002.S0	91.14 ± 0.60	44.88 ± 0.42	11.05 ± 0.21	2449.0 ± 3.1	212.8
MTUA8003.S0	90.06 ± 0.60	44.72 ± 0.42	10.70 ± 0.21	2440.5 ± 3.1	211.4
MTUA8004.S0	89.57 ± 0.60	44.81 ± 0.42	10.44 ± 0.20	2439.5 ± 3.1	210.5
MTUA8005.S0	89.56 ± 0.60	44.28 ± 0.42	9.96 ± 0.20	2434.5 ± 3.1	209.6
Percent Change	-5.2	-4.8	-18.9	-2.2	-3.1

The points plotted in Figure 5 show the trends of the data in Table 5. To make the various trends easier to compare, all of the data were adjusted to make each of the initial values equal to 100. That is, the data in each column of Table 5 were multiplied by the constant that made the first adjusted value equal to 100.

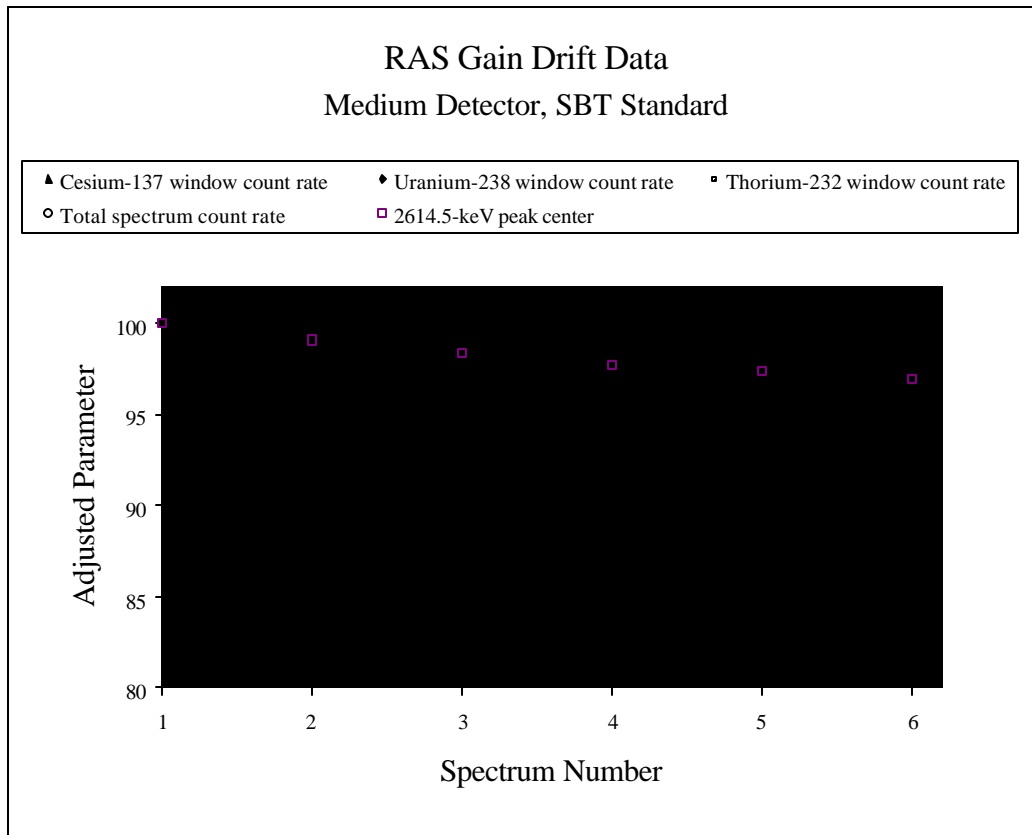


Figure 5. Examples of Parameter Changes Caused by Gain Shift

The largest relative change occurred in the ²³²Th window reading, which was expected because the

²³²Th window is at the high-energy end of the spectrum, where the gain shift has the largest effect, and also because gain changes cause part of the 2614.5-keV “thorium” gamma-ray peak to shift out of the ²³²Th window. The relative changes in the ¹³⁷Cs and ²³⁸U window readings were more moderate, consistent with the positions of these windows near the middle of the spectrum.

Gain shift can cause non-trivial changes in window count rates even if large full energy peaks do not drift in or out of the windows. For example, the entries in Table 5 show that the ²³⁸U window count rate decreased by 4.8 percent during the medium detector calibration measurements with standard SBT. There are no outstanding peaks in the ²³⁸U window (see Figure 4), but gain drift affects the window counts because the background is not constant, but decreases rapidly as the energy increases in this part of the spectrum. At the low-energy end of the ²³⁸U window, the MCA channels contain background counts exceeding 1,080 counts per channel, while on the high end, each channel has only around 320 counts.

The total count readings systematically decreased over the measurement sequence. The net change was about -2.2 percent. The total count points in Figure 5 (circles) suggest that the system efficiency might have drifted downward in the beginning, then started to stabilize.

Points depicted by white-centered squares in Figure 5 show how the center of the 2614.5-keV gamma-ray peak shifted over the measurement sequence.

It is emphasized that the gain shift observed in spectra MTUA8000.S0 through MTUA8005.S0 was not typical, but was the most extreme case observed in the calibration spectra. The other shifts were much smaller, as illustrated, for example, by the shift data in Table 6 for spectra from the SBU standard acquired with the medium detector.

Table 6. Data from a Calibration Measurement Sequence that Showed Typical Gain Shift. The last row in the table shows the net percent change for each parameter.

Spectrum Name	¹³⁷Cs Window (Channels 52-66) Count Rates (c/s)	²³⁸U Window (Channels 139-202) Count Rates (c/s)	²³²Th Window (Channels 203-255) Count Rates (c/s)	Total Count Rates (c/s)	Center of 1764.5-keV Gamma-Ray Peak (Channel Number)
MUSAM000.S0	193.13 ± 0.89	47.80 ± 0.44	1.70 ± 0.08	4297.6 ± 4.2	150.9
MUSAM001.S0	194.60 ± 0.88	47.46 ± 0.44	1.63 ± 0.08	4294.2 ± 4.1	150.7
MUSAM002.S0	195.12 ± 0.88	47.44 ± 0.44	1.62 ± 0.08	4294.6 ± 4.1	150.5
MUSAM003.S0	196.72 ± 0.88	47.33 ± 0.44	1.64 ± 0.08	4294.1 ± 4.1	150.7
MUSAM004.S0	196.52 ± 0.88	46.83 ± 0.43	1.64 ± 0.08	4299.2 ± 4.2	150.5
MUSAM005.S0	196.66 ± 0.88	46.52 ± 0.43	1.65 ± 0.08	4293.9 ± 4.1	150.0
percent change	1.8	-2.7	-2.9	-0.09	-0.6

In the SBU measurement sequence, the gain shift direction may have reversed one or more times. The net effects were essentially negligible, and the window and total count rates display good precision. The difference between the largest and smallest total count rates is only 0.12 percent, and the largest relative

difference between two readings for a particular window count rate is about 5 percent.

Although small gain shifts and stable efficiency characterized most of the sets of calibration measurements, the significant gain drift observed in spectra MTUA8000.S0 through MTUA8005.S0 (Table 5 and Figure 5) is worrisome because the cause is unidentified. As long as the reason for the anomalous behavior remains unknown, nothing can be done to prevent it. The data analysts should watch for evidence of gain and efficiency drifts when analyzing field data, and if significant gain shifts are observed, the analysts should consider the window count rates to be questionable. In these cases, the total count rates will probably be the most reliable data.

6.0 Calibration Measurements

Calibration data were acquired by logging the SBK, SBU, SBT, and SBM standards. Details of the measurements are summarized in Table 7. Table 7 also gives details for the dead time measurements.

The test holes in the calibration standards are not cased, but all of the Hanford boreholes are lined with steel casing. For the great majority of the boreholes, the casing is 6.0 inches in diameter and 0.28 inches thick. To simulate the effects of the most common casing, the calibration measurements with the small and medium detectors were conducted with a 0.28-inch-thick steel sleeve (section of steel pipe) placed over the sonde.

The sleeve was not used for the dead time measurements.

Table 7. Calibration Measurement Parameters

Detector	Calibration Standard	Dead Time Standard	Counting Time Per Spectrum (seconds)	Number of Spectra	0.28-inch-thick Steel Sleeve
Small	SBK		1200	6	used
	SBU		1200	6	used
	SBT		1200	6	used
	SBM		1200	6	used
		SBU	1200	6	not used
		SBL	1200	6	not used
		SBB	1200	6	not used
		SBH	1200	6	not used
Medium	SBK		1000	6	used
	SBU		1000	6	used
	SBT		1000	6	used
	SBM		1000	6	used
		SBU	1000	6	not used
		SBL	1000	6	not used
		SBB	1000	6	not used
		SBH	700	6	not used
Large	SBK		600	6	not used
	SBU		400	6	not used
	SBT		600	7	not used
	SBM		400	6	not used
		SBU	400	6	not used
		SBA	600	6	not used
		SBL	300	6	not used
		SBB	200	6	not used

If it had been certain that monitoring would be limited to logging boreholes and comparing the total or window count rates with the corresponding count rates recorded at earlier times, the calibration measurements would have been made without the steel sleeve. There would have been no need to include the casing effect in the calibration because the casing would not affect the monitoring as long as the casing was not altered (e.g., grouted or replaced with casing of different thickness). However, future analyses of log data might show that the ^{137}Cs or ^{60}Co window count rates, with signals from ^{40}K , ^{238}U , and ^{232}Th removed, can be correlated to in situ concentrations of ^{137}Cs or ^{60}Co . If so, ^{137}Cs and ^{60}Co concentration calculations might be a worthwhile addition to the data analysis. Like any photon scattering medium near the detector, the casing affects the spectral Compton continuum, and thus affects the values of the constants in the algorithm for removal of ^{40}K , ^{238}U , ^{232}Th , and other background signals. Thus, the steel sleeve was used for calibration measurements with the small and medium detectors. The sleeve could not be used for the large detector measurements because the sleeve diameter is too small to accommodate the large detector module.

As indicated earlier, the counts and count rates for eight spectral windows were calculated. Table 8 shows the average window count rates. The window boundaries for these count rate calculations were set manually and individually, *according to energy instead of channel number*. This method of setting

the window boundaries was used to minimize the effects of gain shift.

Table 8. Calibration Count Rate Data

Small Detector Calibration Data									
Window Names and Count Rates in counts/second									
Standard	Lithology	Cs-137	Mid-Range	Pa-234	Co-60	K-40	U-238	Th-232	Total
SBK	22.120 ± 0.086	1.401 ± 0.049	1.062 ± 0.025	0.510 ± 0.060	0.945 ± 0.069	0.446 ± 0.021	0.066 ± 0.022	0.008 ± 0.007	26.56 ± 0.17
SBU	873.6 ± 6.8	39.5 ± 3.2	24.00 ± 0.94	9.3 ± 1.0	19.37 ± 0.58	6.60 ± 0.24	7.39 ± 0.12	0.187 ± 0.036	979.9 ± 3.9
SBT	355.1 ± 5.3	12.6 ± 3.3	9.15 ± 0.64	3.43 ± 0.41	5.79 ± 0.27	3.10 ± 0.16	7.50 ± 0.42	1.24 ± 0.10	398.0 ± 1.8
SBM	781.5 ± 7.4	35.6 ± 4.5	22.5 ± 1.2	8.58 ± 0.98	16.28 ± 0.41	6.45 ± 0.30	9.52 ± 0.45	0.921 ± 0.071	881.4 ± 3.7
Medium Detector Calibration Data									
Window Names and Count Rates in counts per second									
Standard	Lithology	Cs-137	Mid-Range	Pa-234	Co-60	K-40	U-238	Th-232	Total
SBK	95.11 ± 0.84	6.79 ± 0.18	5.22 ± 0.12	2.570 ± 0.084	5.18 ± 0.16	2.12 ± 0.33	0.337 ± 0.018	0.026 ± 0.012	117.35 ± 0.68
SBU	3714 ± 14	215 ± 16	122.9 ± 1.4	50.8 ± 4.9	106.2 ± 4.3	36.5 ± 2.3	48.61 ± 0.99	1.57 ± 0.10	4295.6 ± 4.5
SBT	1523 ± 13	66.5 ± 9.3	51.6 ± 3.2	17.2 ± 1.5	28.9 ± 1.4	15.75 ± 0.96	38.79 ± 0.74	9.98 ± 0.56	1751.9 ± 4.0
SBM	3307.0 ± 7.3	197.8 ± 1.5	116.6 ± 1.0	45.9 ± 3.6	87.5 ± 3.3	34.8 ± 2.0	55.7 ± 1.0	7.49 ± 0.22	3852.8 ± 5.6
Large Detector Calibration Data									
Window Names and Count Rates in counts per second									
Standard	Lithology	Cs-137	Mid-Range	Pa-234	Co-60	K-40	U-238	Th-232	Total
SBK	1406 ± 24	155 ± 10	125.9 ± 4.5	67.4 ± 5.1	152.0 ± 9.3	138.5 ± 8.4	16.39 ± 0.39	1.621 ± 0.099	2062 ± 24
SBU	43977 ± 794	5929 ± 335	4304 ± 156	2154 ± 37	4680 ± 163	1881 ± 103	3359 ± 351	305 ± 66	66590 ± 502
SBT	21820 ± 110	2172 ± 33	1845.0 ± 3.4	725 ± 31	1081.7 ± 8.5	530.3 ± 3.1	1282.8 ± 2.3	466 ± 23	29923 ± 154
SBM	40482 ± 54	5478 ± 59	4050 ± 30	2001 ± 14	3969 ± 22	1649 ± 12	3165 ± 21	618.0 ± 7.2	61411 ± 172

7.0 Spectrum Stripping Methods

The derivation of the computational method for subtracting ^{40}K , ^{238}U , and ^{232}Th signals from the count or count rate in any portion of a spectrum is straightforward. The spectrum portion of interest might be the ^{137}Cs window, the ^{60}Co window, another window, the filtered spectrum, or even the entire

spectrum. The method is similar, though not identical, to methods developed for potassium-uranium-thorium analyses in the uranium (Stromswold and Kosanke 1978; Evans et al. 1979; Wilson and Stromswold 1981) and petroleum (Lock and Hoyer 1971; Wichmann et al. 1975; Mathis et al. 1984; Koizumi 1988) industries. The subtraction of background counts from portions of spectra has been called “spectrum window stripping,” “window stripping,” or “stripping.”

The first example to be considered is full spectrum stripping. The assumption is that the total count rate for the whole spectrum contains background contributions from the natural sources, ^{40}K , ^{238}U , and ^{232}Th , mixed with contributions from a source in process waste, such as ^{137}Cs . Spectral background contributions include full energy peaks and Compton continuums, and any other features, such as escape peaks, backscatter peaks, and sum peaks. The objective is to strip the background signals from spectra to isolate the total count rates due to the sources in process waste. If just one process waste source is present, it may be possible to relate the stripped total count rate to the source concentration.

If R represents the total spectral count rate measured with only ^{40}K , ^{238}U , and ^{232}Th present, and if C_K , C_U , and C_T are the ^{40}K , ^{238}U , and ^{232}Th concentrations, then

$$D_1 \cdot C_K + D_2 \cdot C_U + D_3 \cdot C_T = R \quad \text{Eq. (2)}$$

states that the total count rate is a linear combination of the three source concentrations. D_1 , D_2 , and D_3 are the proportionality constants.

Calibration measurements have been made with three standards, SBK, SBU, and SBT; therefore, there are three sets of concentrations and three average spectral count rates. The three equations containing these factors can be written in matrix notation:

$$\begin{bmatrix} C_{K1} & C_{U1} & C_{T1} \\ C_{K2} & C_{U2} & C_{T2} \\ C_{K3} & C_{U3} & C_{T3} \end{bmatrix} \begin{bmatrix} D_1 \\ D_2 \\ D_3 \end{bmatrix} = \begin{bmatrix} R_1 \\ R_2 \\ R_3 \end{bmatrix}. \quad \text{Eq. (3)}$$

Then the proportionality, or stripping, factors can be calculated by

$$\begin{bmatrix} D_1 \\ D_2 \\ D_3 \end{bmatrix} = \begin{bmatrix} C_{K1} & C_{U1} & C_{T1} \\ C_{K2} & C_{U2} & C_{T2} \\ C_{K3} & C_{U3} & C_{T3} \end{bmatrix}^{-1} \begin{bmatrix} R_1 \\ R_2 \\ R_3 \end{bmatrix} \quad \text{Eq. (4)}$$

because all of the concentrations are known and the window count rates can be calculated from the recorded spectral data.

The 3×3 matrix with the ^{40}K , ^{238}U , and ^{232}Th concentrations of SBK, SBU, and SBT is (all

concentrations expressed in picocuries per gram),

$$\begin{bmatrix} C_{K,SBK} & C_{U,SBK} & C_{T,SBK} \\ C_{K,SBU} & C_{U,SBU} & C_{T,SBU} \\ C_{K,SBT} & C_{U,SBT} & C_{T,SBT} \end{bmatrix} = \begin{bmatrix} 53.5 & 1.16 & 0.11 \\ 10.72 & 190.52 & 0.66 \\ 10.63 & 10.02 & 58.11 \end{bmatrix} \quad \text{Eq. (5)}$$

and the inverse matrix is

$$\begin{bmatrix} C_{K,SBK} & C_{U,SBK} & C_{T,SBK} \\ C_{K,SBU} & C_{U,SBU} & C_{T,SBU} \\ C_{K,SBT} & C_{U,SBT} & C_{T,SBT} \end{bmatrix}^{-1} = \begin{bmatrix} 1.87E-2 & -1.12E-4 & -3.42E-5 \\ -1.04E-3 & 5.26E-3 & -5.77E-5 \\ -3.24E-3 & -8.86E-4 & 1.72E-2 \end{bmatrix}. \quad \text{Eq. (6)}$$

The full spectrum stripping factors in Table 9 were calculated by substituting this inverse matrix and the measured (average) total count rates for the three standards (Table 8) into Equation (4).

Table 9. Full Spectrum Stripping Factors

Detector	D_1 (counts/second) per (pCi/g)	D_2 (counts/second) per (pCi/g)	D_3 (counts/second) per (pCi/g)
Small	0.374	5.10	5.99
Medium	1.65	22.4	26.4
Large	30.1	346	456

The *uncertainties* for the stripping factors have not been calculated because the propagation-of-uncertainty equations for matrix inversion are very complicated and it is not known at this time if the stripping will yield useful results. Expressions for the uncertainties will be derived later if experiments with field data indicate that accurate source concentrations can in fact be calculated from the stripped spectral count rates.

The use of these stripping factors can be demonstrated with measurements from the SBM standard, which were not used in the stripping factor derivations. The stripping factors and the known ^{40}K , ^{238}U , and ^{232}Th concentrations for the SBM calibration standard can be substituted into Equation (2) to calculate the expected background K-U-Th count rates. Because SBM contains no sources in addition to ^{40}K , ^{238}U , and ^{232}Th , the background count rates should be equal to the actual count rates. The predicted and measured total count rates are displayed in Table 10. Each prediction agrees with its measured counterpart to within 2 percent.

Table 10. Total Count Rate Stripping Demonstration

Detector	Predicted SBM Total Count Rates (counts/second)	Measured SBM Total Count Rates (counts/second)	Residual $\frac{(measured - predicted) \times 100}{(measured)}$
Small	892	881.4 ± 3.7	-1.2%
Medium	3914	3852.8 ± 5.6	-1.6%
Large	62665	61411 ± 172	-2.0%

The spectral stripping discussion makes no mention of the Z effect because potassium has too low a Z value ($Z = 19$) to produce a Z anomaly, and the concentrations of natural uranium and thorium in the calibration standards and in the subsurface at Hanford are too low to make Z significantly different from the normal value. Conceivable concentrations of ^{137}Cs , ^{60}Co , ^{154}Eu , and other common process waste constituents will also be too low to affect Z. The Z effect on measurements might not be negligible, however, when zones containing high concentrations of processed uranium are logged. Spectra from those relatively infrequent encounters with high concentrations of processed uranium should be filtered (by deleting the spectral component below 570 keV), then stripped.

Stripping factors for filtered spectra are derived by the same method as used for total count rates, except the filtered count rates are used instead of the total count rates in Equation (4). The filtered spectrum stripping factors are listed in Table 11.

Table 11. Filtered Spectrum Stripping Factors

Detector	D_1 (counts/second) per (pCi/g)	D_2 (counts/second) per (pCi/g)	D_3 (counts/second) per (pCi/g)
Small	0.0697	0.552	0.644
Medium	0.343	3.02	3.42
Large	9.48	118	120

Table 12 shows the measured filtered count rates for standard SBM compared to the count rates predicted using the filtered stripping factors.

Table 12. Filtered Count Rate Stripping Demonstration

Detector	Predicted SBM Filtered Count Rates (counts/second)	Measured SBM Filtered Count Rates (counts/second)	Residual $\frac{(measured - predicted) \times 100}{(measured)}$
Small	97.5	99.9 ± 5.3	2.4%
Medium	528.5	545.8 ± 2.8	3.2%
Large	19883	20930 ± 162	5.0%

Another data processing method that might be useful is ^{137}Cs window stripping. The ^{137}Cs spectral window extends from 570 to 740 keV (Table 2). Some gamma rays from nuclides in the uranium series

(e.g., ^{214}Bi [609.3 keV]) and nuclides in the thorium series (e.g., ^{228}Ac [794.8 keV], ^{212}Bi [727.2 keV], ^{208}Tl [583.1 keV]) will contribute full-energy peak counts directly to this window. Gamma rays from other nuclides (e.g., ^{40}K [1460.8 keV], ^{214}Bi [1120.3 keV, 1764.5 keV, and 2204.1 keV], ^{228}Ac [911.1 keV], ^{208}Tl [860.5 and 2614.5 keV]) have energies that are higher than the upper end of the ^{137}Cs window; therefore, the Compton continuums for these gamma rays will add counts to the ^{137}Cs window. Because the stripping method accounts for all of these potential contributions, the stripping constants can be calculated by substituting the ^{137}Cs window count rates into Equation (4). Table 13 lists the constants. As before, the constants can be tested by calculating the ^{137}Cs window count rates for the SBM standard and comparing the predicted count rates with the measured count rates. Results are displayed in Table 14.

Table 13. Spectrum Stripping Factors for the ^{137}Cs Window

Detector	D_1 (counts/second) per (pCi/g)	D_2 (counts/second) per (pCi/g)	D_3 (counts/second) per (pCi/g)
Small	0.0214	0.205	0.183
Medium	0.101	1.12	0.955
Large	2.15	30.9	32.2

Table 14. ^{137}Cs Window Count Rate Stripping Demonstration

RAS Detector	Predicted SBM ^{137}Cs Window Count Rates (counts/second)	Measured SBM ^{137}Cs Window Count Rates (counts/second)	Residual $\frac{(\text{measured} - \text{predicted}) \times 100}{(\text{measured})}$
Small	33.9	35.6 ± 4.5	4.8%
Medium	182	197.8 ± 1.5	8.0%
Large	5233	5478 ± 59	4.5%

In theory, the total ^{40}K , ^{238}U , and ^{232}Th contribution to the ^{137}Cs window count rate can be subtracted from the measured ^{137}Cs window count rate, and the residual, or stripped, window count rate should be proportional to the ^{137}Cs concentration. This would mean that the ^{137}Cs concentration could be calculated from the stripped count rate if the proportionality constant, or ^{137}Cs calibration factor, were known. This hypothesis cannot be tested with calibration data because none of the calibration standards contain ^{137}Cs . Therefore, the hypothesis will have to be confirmed (or invalidated) through analyses of Hanford field spectra.

The stripping factors for the ^{60}Co window were also calculated. The values are shown in Table 15.

Table 15. Spectrum Stripping Factors for the ^{60}Co Window

Detector	D_1 (counts/second) per (pCi/g)	D_2 (counts/second) per (pCi/g)	D_3 (counts/second) per (pCi/g)
Small	0.0153	0.101	0.0825
Medium	0.0841	0.551	0.403
Large	2.28	24.4	14.5

The two ^{60}Co gamma rays have energies (1173.2 and 1332.5 keV) that are higher than the upper edge of the ^{137}Cs window (740 keV), so if ^{60}Co coexists with ^{137}Cs , the Compton continuums associated with the two gamma rays will add counts to the ^{137}Cs window. Therefore, when ^{60}Co coexists with ^{137}Cs , the ^{60}Co contribution to the ^{137}Cs window must be determined and subtracted before the ^{137}Cs concentration is calculated. Data to determine the stripping factor for the ^{60}Co contribution to the ^{137}Cs window cannot be recorded with calibration measurements because the calibration models do not contain ^{60}Co . Laboratory measurements with ^{60}Co button sources would be inappropriate because the spectra for point sources will have different Compton continuums than spectra from distributed sources. The stripping factor will therefore have to be derived from field spectra that contain varying signals from ^{60}Co , but negligible signals from ^{137}Cs .

If the uses of the ^{137}Cs and ^{60}Co window count rates are pursued, the baseline data will be used to identify boreholes that penetrate depth increments with appropriate concentrations of ^{137}Cs and ^{60}Co . These sections will be logged with the RAS, then the relationships between stripped ^{137}Cs (or ^{60}Co) window count rate and ^{137}Cs (or ^{60}Co) concentration will be derived. These relationships will be the ^{137}Cs and ^{60}Co calibrations.

Because the borehole logging and the associated data analyses will take months to complete, these activities are not considered part of the RAS calibration. The approaches outlined in Section 7.0, "Spectrum Stripping Methods," should be regarded as a roadmap for the development of potentially useful analysis methods.

Determination of natural background signals for stripping requires the ^{40}K , ^{238}U , and ^{232}Th concentrations, C_K , C_U , and C_T . For the present, these concentrations should be taken from the SGLS baseline data.

Intuition might suggest that the ^{40}K , ^{238}U , and ^{232}Th concentrations can be calculated directly from the RAS spectra when ^{137}Cs and/or ^{60}Co are the only contaminants present. The ^{137}Cs and ^{60}Co gamma rays have energies (661.6 keV, 1173.2 keV, and 1332.5 keV) that lie below the lower edge of the ^{40}K window (1390 keV); therefore, the counts in the ^{40}K , ^{238}U , and ^{232}Th windows should be nearly free of contributions from ^{137}Cs and ^{60}Co . Thus, the ^{40}K , ^{238}U , and ^{232}Th concentrations could be calculated by the method developed for the NURE (Stromswold and Kosanke 1978; Evans et al. 1979; Wilson and Stromswold 1981).

The NURE method is based on the proposition that each window count rate is a linear combination of

the three concentrations. For example,

$$R_K = A_{1K} \cdot C_K + A_{2K} \cdot C_U + A_{3K} \cdot C_T , \quad \text{Eq. (7)}$$

expresses the count rate in the ^{40}K window, R_K , in terms of the three concentrations, C_K , C_U , and C_T , and three proportionality constants A_{1K} , A_{2K} , and A_{3K} . This equation and the two similar equations for the count rates in the ^{238}U and ^{232}Th windows make a set of three equations,

$$\begin{bmatrix} R_K \\ R_U \\ R_T \end{bmatrix} = \begin{bmatrix} A_{1K} & A_{2K} & A_{3K} \\ A_{1U} & A_{2U} & A_{3U} \\ A_{1T} & A_{2T} & A_{3T} \end{bmatrix} \begin{bmatrix} C_K \\ C_U \\ C_T \end{bmatrix} , \quad \text{Eq. (8)}$$

for a measurement in one calibration standard. Equations for measurements in three calibration standards can be written in matrix notation as

$$[R] = [A][C] , \quad \text{Eq. (9)}$$

in which $[R]$, $[A]$, and $[C]$ are 3×3 matrices. The elements of $[R]$ are measured window count rates, the elements of $[C]$ are ^{40}K , ^{238}U , and ^{232}Th calibration standard concentrations, and the elements of $[A]$ are the proportionality constants.

Clearly, the elements of $[A]$ can be calculated from the count rate matrix and the inverse of the concentration matrix:

$$[A] = [R][C]^{-1} . \quad \text{Eq. (10)}$$

If the elements of $[A]$ are known, then the elements of $[A]^{-1}$ can be determined. $[A]^{-1}$ is the *calibration matrix*, which is evident from the equation obtained by multiplying both sides of Equation (8) by $[A]^{-1}$:

$$\begin{bmatrix} C_K \\ C_U \\ C_T \end{bmatrix} = [A]^{-1} \begin{bmatrix} R_K \\ R_U \\ R_T \end{bmatrix} . \quad \text{Eq. (11)}$$

Equation (11) indicates that the three concentrations can be calculated from three recorded window count rates.

This method works well for the K-U-Th analyses performed in the petroleum and mineral industries, but it might not be generally applicable to spectra that contain signals from process waste contaminants. This indication comes from analysis of a spectrum (m6mci025.chn) that was recorded during the 1996 GJO tests by placing a 6-mCi ^{137}Cs button source near the RAS medium detector.

The dead time for m6mci025.chn was small, 0.44 percent; therefore, the gamma flux was weak compared to the fluxes that will be encountered when logging ^{137}Cs -rich zones at Hanford. What is worrisome is that upscatter from this relatively weak ^{137}Cs source apparently put 0.26 c/s in the ^{40}K window, 0.36 c/s in the ^{238}U window, and 0.04 c/s in the ^{232}Th window. These window count rates are not greatly different from the window count rates that will be recorded at Hanford for the natural background. For the nominal Hanford concentrations of 15 pCi/g ^{40}K , 1 pCi/g ^{238}U , and 1 pCi/g ^{232}Th , the calibration data and the window stripping method lead to count rate estimates of 1 c/s in the ^{40}K window, 0.9 c/s in the ^{238}U window, and 0.2 c/s in the ^{232}Th window. The implication is that the ^{137}Cs concentration will not have to rise too high before the counts in the three windows due to ^{137}Cs are higher than the counts due to ^{40}K , ^{238}U , and ^{232}Th . Obviously, if the count rates in the three windows are not entirely due to ^{40}K , ^{238}U , and ^{232}Th , then the calculated concentrations, C_K , C_U , and C_T , will be incorrect, and any stripping based on these concentrations will also be incorrect.

The experimental circumstances under which m6mci025.chn was acquired were not documented; therefore, it is possible that the spectrum was recorded without adequate shielding to stop natural background gamma rays from reaching the detector. If this were the case, then the counts in the ^{40}K , ^{238}U , and ^{232}Th windows might represent background instead of upscatter from the 661.6-keV ^{137}Cs gamma rays. After the RAS is deployed at Hanford, the upscatter phenomenon will be studied through examination of field data from ^{137}Cs -contaminated zones.

8.0 Preliminary Field Verification Acceptance Criteria

During field operations, spectra will be regularly recorded with a field verification source mounted on the RAS sonde. Total counts and selected window counts will be calculated and compared to acceptance criteria to confirm that the data acquisition system is operating properly.

Similar tests are routinely performed with the SGLSs. The SGLS field verification measurements and gamma-ray sources for these measurements are described by Koizumi (1996).

A field verification source was procured from AEA Technology specifically for RAS measurements. The source product name is *KUTh Field Verifier* and the product code number is 188701. The source contains ^{40}K , ^{238}U , and its decay progenies (the source contains ^{235}U also, but this nuclide does not contribute to field verification measurements), and ^{232}Th and its decay progenies; the concentrations are consistent with the following decay activities (determined on December 12, 2000):

^{40}K 1.663 microcuries
 ^{238}U 0.46 microcuries
 ^{232}Th 0.331 microcuries.

The long half lives of these nuclides (^{40}K , 1.3×10^9 years; ^{238}U , 4.5×10^9 years; ^{232}Th , 1.4×10^{10} years) ensure that the decay activities can be regarded as practically stable. The decay progenies of ^{238}U and ^{232}Th are also assumed to be present in quantities consistent with decay equilibrium. Thus, there is no expectation of any increase in gamma-ray output associated with a buildup of gamma-ray-emitting decay products such as ^{214}Bi (decay product of ^{238}U) and ^{208}Tl (decay product of ^{232}Th).

Field verification acceptance criteria will be derived through normal control chart methods. Many spectra will be acquired, then total counts and spectral window counts will be statistically analyzed. Acceptance criteria will be expressed as *warning limits* and *control limits*. If a set of counts or count rates for a particular window has a mean $\langle R \rangle$ and a standard deviation SR , the warning limits for a new measurement are $\langle R \rangle - 2SR$ and $\langle R \rangle + 2SR$, and the control limits are $\langle R \rangle - 3SR$ and $\langle R \rangle + 3SR$. According to these expressions, a new reading exceeds the warning limit if it lies outside of the 95-percent confidence interval (differs from the mean by more than two standard deviations), and the reading exceeds the control limit if it lies outside of the 99-percent confidence interval (differs from the mean by more than three standard deviations).

Koizumi (1999) describes the analogous limits for the SGLSs.

Early in 2001, the KUTh source was used to collect 11 spectra with the RAS small detector, 11 with the medium detector, and 12 with the large detector. Because these numbers of verification spectra are small (less than 30), the field verification acceptance limits are expressed in a slightly different way, and should be considered preliminary:

$$\begin{aligned}\text{lower limit} &= \langle R \rangle - t \cdot SR \\ \text{upper limit} &= \langle R \rangle + t \cdot SR.\end{aligned}$$

In these limit expressions, t is the critical value for the quantity in Student's t -distribution (Johnson 1992) known as the t -statistic. These critical values depend on the number of samples and the confidence intervals. For example, the critical value of t for the 95-percent confidence interval satisfies

$$\int_{x=-t}^{x=+t} f(x)dx = 0.95, \quad \text{Eq. (12)}$$

meaning that 95 percent of the area under the t -distribution function, $f(x)$, lies between $x = -t$ and $x = +t$. The distribution function, which is normalized and symmetric about $x = 0$, is

$$f(x) = \frac{1}{\sqrt{np}} \frac{\Gamma\left(\frac{n+1}{2}\right)}{\Gamma\left(\frac{n}{2}\right)} \left(1 + \frac{x^2}{n}\right)^{-\left(\frac{n+1}{2}\right)}. \quad \text{Eq. (13)}$$

In the above equation

$$\Gamma(n) \equiv \int_0^{\infty} e^{-x} x^{n-1} dx, \quad \text{Eq. (14)}$$

and n is the number of samples.

The critical values of t that were used to formulate acceptance criteria are tabulated in Table 16.

Table 16. Critical Values of t for the 95 and 99 Percent Confidence Intervals

n	Confidence Interval	Critical t Value
11	95 percent	2.201
11	99 percent	3.106
12	95 percent	2.179
12	99 percent	3.055

Every spectrum was acquired over a 1,000-second counting time.

Table 17 shows the field verifier count data for the RAS small detector. The acceptance criteria in counts for this detector are listed in Table 18, and the criteria in count rates are listed in Table 19.

Table 17. Field Verifier Count Data for the RAS Small Detector

Window Name	Window Boundaries (MCA Channels)	Count Mean (counts)	Count Standard Deviation (counts)
S1 (Lithology)	0-51	107968	571
S2 (Cesium-137)	52-66	5581	153
S3 (Mid-Range)	67-83	3267	59
S4 (Protactinium-234)	84-93	1378	66
S5 (Cobalt-60)	94-121	2517	47
S6 (Potassium-40)	122-138	1152	41
S7 (Uranium-238)	139-202	1409	61
S8 (Thorium-232)	203-255	188	14
Total Spectrum Count	0-255	123459	690

Table 18. Count Acceptance Criteria for the RAS Small Detector

Window Name	Lower Control Limit (counts)	Lower Warning Limit (counts)	Upper Warning Limit (counts)	Upper Control Limit (counts)
S1 (Lithology)	106195	106711	109224	109741
S2 (Cesium-137)	5106	5244	5917	6056
S3 (Mid-Range)	3083	3137	3397	3450
S4 (Protactinium-234)	1173	1233	1523	1583
S5 (Cobalt-60)	2370	2413	2620	2663
S6 (Potassium-40)	1025	1062	1243	1280
S7 (Uranium-238)	1219	1274	1544	1599
S8 (Thorium-232)	145	158	218	230
Total Spectrum Count	121316	121941	124978	125602

Table 19. Count Rate Acceptance Criteria for the RAS Small Detector

Window Name	Lower Control Limit (counts/second)	Lower Warning Limit (counts/second)	Upper Warning Limit (counts/second)	Upper Control Limit (counts/second)
S1 (Lithology)	106.195	106.711	109.224	109.741
S2 (Cesium-137)	5.106	5.244	5.917	6.056
S3 (Mid-Range)	3.083	3.137	3.397	3.450
S4 (Protactinium-234)	1.173	1.233	1.523	1.583
S5 (Cobalt-60)	2.370	2.413	2.620	2.663
S6 (Potassium-40)	1.025	1.062	1.243	1.280
S7 (Uranium-238)	1.219	1.274	1.544	1.599
S8 (Thorium-232)	0.145	0.158	0.218	0.230
Total Spectrum Count	121.316	121.941	124.978	125.602

Table 20 shows the field verifier count data for the RAS medium detector. The acceptance criteria in counts for this detector are listed in Table 21, and the criteria in count rates are listed in Table 22.

Table 20. Field Verifier Count Data for the RAS Medium Detector

Window Name	Window Boundaries (MCA Channels)	Count Mean (counts)	Count Standard Deviation (counts)
M1 (Lithology)	0-51	281315	1549
M2 (Cesium-137)	52-66	16884	408
M3 (Mid-Range)	67-83	10036	99
M4 (Protactinium-234)	84-93	4130	166
M5 (Cobalt-60)	94-121	7673	100
M6 (Potassium-40)	122-138	3822	169
M7 (Uranium-238)	139-202	4596	132
M8 (Thorium-232)	203-255	916	51
Total Spectrum Count	0-255	329372	2022

Table 21. Count Acceptance Criteria for the RAS Medium Detector

Window Name	Lower Control Limit (counts)	Lower Warning Limit (counts)	Upper Warning Limit (counts)	Upper Control Limit (counts)
M1 (Lithology)	276504	277905	284724	286126
M2 (Cesium-137)	15615	15985	17783	18152
M3 (Mid-Range)	9729	9818	10254	10343
M4 (Protactinium-234)	3616	3765	4494	4644
M5 (Cobalt-60)	7363	7453	7893	7984
M6 (Potassium-40)	3296	3449	4194	4347
M7 (Uranium-238)	4187	4306	4886	5005
M8 (Thorium-232)	759	805	1028	1073
Total Spectrum Count	323093	324922	333821	335650

Table 22. Count Rate Acceptance Criteria for the RAS Medium Detector

Window Name	Lower Control Limit (counts/ second)	Lower Warning Limit (counts/ second)	Upper Warning Limit (counts/ second)	Upper Control Limit (counts/ second)
M1 (Lithology)	276.504	277.905	284.724	286.126
M2 (Cesium-137)	15.615	15.985	17.783	18.152
M3 (Mid-Range)	9.729	9.818	10.254	10.343
M4 (Protactinium-234)	3.616	3.765	4.494	4.644
M5 (Cobalt-60)	7.363	7.453	7.893	7.984
M6 (Potassium-40)	3.296	3.449	4.194	4.347
M7 (Uranium-238)	4.187	4.306	4.886	5.005
M8 (Thorium-232)	0.759	0.805	1.028	1.073
Total Spectrum Count	323.093	324.922	333.821	335.650

Table 23 shows the field verifier count data for the RAS large detector. The acceptance criteria in counts for this detector are listed in Table 24, and the criteria in count rates are listed in Table 25.

Table 23. Field Verifier Count Data for the RAS Large Detector

Window Name	Window Boundaries (MCA Channels)	Count Mean (counts)	Count Standard Deviation (counts)
L1 (Lithology)	0-50	861259	6276
L2 (Cesium-137)	51-64	96026	2227
L3 (Mid-Range)	65-82	70516	353
L4 (Protactinium-234)	83-92	29541	1027
L5 (Cobalt-60)	93-121	55722	268
L6 (Potassium-40)	122-139	33568	855
L7 (Uranium-238)	140-209	37668	459
L8 (Thorium-232)	210-255	10808	239
Total Spectrum Count	0-255	1195108	7995

Table 24. Count Acceptance Criteria for the RAS Large Detector

Window Name	Lower Control Limit (counts)	Lower Warning Limit (counts)	Upper Warning Limit (counts)	Upper Control Limit (counts)
L1 (Lithology)	842088	847584	874934	880430
L2 (Cesium-137)	89224	91174	100879	102829
L3 (Mid-Range)	69437	69746	71286	71596
L4 (Protactinium-234)	26403	27302	31779	32679
L5 (Cobalt-60)	54903	55138	56306	56541
L6 (Potassium-40)	30957	31706	35430	36178
L7 (Uranium-238)	36266	36668	38668	39070
L8 (Thorium-232)	10077	10287	11329	11539
Total Spectrum Count	1170688	1177689	1212527	1219528

Table 25. Count Rate Acceptance Criteria for the RAS Large Detector

Window Name	Lower Control Limit (counts/second)	Lower Warning Limit (counts/second)	Upper Warning Limit (counts/second)	Upper Control Limit (counts/second)
L1 (Lithology)	842.09	847.58	874.93	880.43
L2 (Cesium-137)	89.22	91.17	100.88	102.83
L3 (Mid-Range)	69.44	69.75	71.29	71.60
L4 (Protactinium-234)	26.40	27.30	31.78	32.68
L5 (Cobalt-60)	54.90	55.14	56.31	56.54
L6 (Potassium-40)	30.96	31.71	35.43	36.18
L7 (Uranium-238)	36.27	36.67	38.67	39.07
L8 (Thorium-232)	10.08	10.29	11.33	11.54
Total Spectrum Count	1170.69	1177.69	1212.53	1219.53

At the beginning of the monitoring project, system tests will be based on readings from three windows: the ^{40}K window, the ^{238}U window, and the total spectrum count window. The ^{40}K window is narrow and the count (or count rate) will be sensitive to the position of the 1460.8-keV gamma-ray peak within the window. The window count (or count rate) should therefore provide a measure of the system gain stability. The ^{238}U window is wider, and the counts (or count rates) should be somewhat dependent on the system gain and efficiency. The total spectrum count is expected to be relatively insensitive to gain shift, but sensitive to changes in system efficiency.

Field verifier spectra will be recorded at the beginning and end of each day, and when detectors are changed. The ^{40}K , ^{238}U , and total spectrum counts (or count rates) will be calculated and compared with the appropriate warning and control limits. The outcomes of these comparisons are listed in Table 26.

Table 26. Outcomes of Field Verification Measurements

Test Result	Outcome
The counts (or count rates) for all three windows lie within warning limits.	The system passes the acceptance test.
One or more of the count (or count rate) readings exceeds the warning limits, but not the control limits.	The outcome depends on data from the next (followup) field verification spectrum. Outcomes are listed in Table 27.
One or more count (or count rate) readings exceeds the control limits.	The system fails the acceptance test.

Table 27. Outcomes of Followup Field Verification Measurements

Test Result	Outcome
The counts (or count rates) for all three windows lie within warning limits.	The system passes the acceptance test.
The count (or count rate) reading that exceeded the warning limit in the earlier measurement now falls within the warning limits, but a different count (or count rate) now falls outside of the warning limits, but not the control limits.	Data from the next (third) field verification spectrum are analyzed, and this table is used to determine the outcome.
The count (or count rate) reading that exceeded the warning limit in the earlier measurement exceeds the warning limit again, and lies on the same side of the data set mean as before.	The system fails the acceptance test.
The count (or count rate) reading that exceeded the warning limit in the earlier measurement exceeds the warning limit again, but lies on the opposite side of the data set mean.	Data from the next (third) field verification spectrum are analyzed, and this table is used to determine the outcome.
One or more count (or count rate) readings exceeds the control limits.	The system fails the acceptance test.

The Hanford Office Technical Lead should be notified of an acceptance test failure as soon as possible so that the cause of the failure can be determined and corrected.

9.0 Acknowledgments

Mr. R.G. McCain formulated the preliminary field verification criteria.

Ms. R.M. Paxton prepared this report for publication.

10.0 References

Crew, M.E., 1979. *MULTIPIT, A method for Calibration of Logging Systems*, Paper II, Twentieth Annual Logging Symposium Transactions, Society of Professional Well Log Analysts, June 1979, Tulsa, Oklahoma.

Evans, H.B., D.C. George, J.W. Allen, B.N. Key, D.L. Ward, and M.A. Mathews, 1979. *A Borehole Gamma-Ray Spectrometer for Uranium Exploration*, Paper X, Twentieth Annual Logging Symposium Transactions, Society of Professional Well Log Analysts, June 1979, Tulsa, Oklahoma.

Heistand, B.E., and E.F. Novak, 1984. *Parameter Assignments for Spectral Gamma-Ray Borehole Calibration Models*, GJBX-2(84), prepared by Bendix Field Engineering Corporation for the U.S. Department of Energy Grand Junction Projects Office, Grand Junction, Colorado.

Isaacson, R.E., 1982. *Supporting Information for the Scientific Basis for Establishing Dry-Well Monitoring Frequencies*, RHO-RE-EV-4, prepared by Rockwell Hanford Operations for the U.S. Department of Energy Richland Operations Office, Richland, Washington.

Johnson, R., 1992. *Elementary Statistics* (Sixth Edition), Duxbury Press, Belmont, California.

Knoll, G.F., 2000. *Radiation Detection and Measurement* (Third Edition), John Wiley and Sons, Inc., New York.

Koizumi, C.J., 1988. *Computer Determination of Calibration and Environmental Corrections for a Natural Spectral Gamma Ray Logging System*, SPE Formation Evaluation, September 1988.

_____, 1996. *Vadose Zone Characterization Project at the Hanford Tank Farms Biannual Recalibration of Two Spectral Gamma-Ray Logging System Used for Baseline Characterization Measurements in the Hanford Tank Farms*, DOE/ID/12584-266 GJPO-HAN-3, prepared by Rust Geotech, Inc., for the U.S. Department of Energy Grand Junction Office, Grand Junction, Colorado.

_____, 1999. *Hanford Tank Farms Vadose Zone Sixth Recalibration of Spectral Gamma-Ray Logging Systems Used for Baseline Characterization Measurements in the Hanford Tank Farms*, GJO-99-100-TAR GJO-HAN-26, prepared by MACTEC-ERS for the U.S. Department of Energy Grand Junction Office, Grand Junction, Colorado.

Leino, R., D.C. George, B.N. Key, L. Knight, and W.D. Steele, 1994. *Field Calibration Facilities for Environmental Measurements of Radium, Thorium, and Potassium*, DOE/ID/12584-179 GJ/TMC-01 (Third Edition) UC-902, Prepared by Rust Geotech, Inc., for the U.S. Department of Energy Grand Junction Office, Grand Junction, Colorado.

Lock, G.A., and Hoyer, W.A., 1971. *Natural Gamma Ray Spectral Logging*, The Log Analyst, Vol. XII, No. 5, October 1971.

Mathis, G.L., C.W. Tittle, D.R. Rutledge, R. Mayer, and W.E. Ferguson, 1984. *A Spectral Gamma Ray (SGRTM) Tool*, Society of Professional Well Log Analysts Twenty-Fifth Annual Logging Symposium Transactions, Paper W, New Orleans, Louisiana, June 1984.

Steele, W.D., and D.C. George, 1986, *Field Calibration Facilities for Environmental Measurement of Radium, Thorium, and Potassium*, GJ/TMC-01 (Second Edition) UC-70A, Prepared by Bendix Field Engineering Corp. for the U.S. Department of Energy Grand Junction Projects Office, Grand Junction, Colorado.

Stromswold, D.C., and K.L. Kosanke, 1978. *Calibration and Error Analysis for Spectral Radiation Detectors*, IEEE Transactions on Nuclear Science, Vol. N5-25, No. 1.

Trahey, N.M., A.M. Voeks, and M.D. Soriano, 1982. *Grand Junction/New Brunswick Laboratory Interlaboratory Measurement Program, Part I: Evaluation, Part II: Methods Manual*, Report NBL-303, New Brunswick Laboratory, Argonne, Illinois.

Wichmann, P.A., V.C. McWhirter, and E.C. Hopkinson, 1975. *Field Results of the Natural Gamma Ray Spectralog*, Society of Professional Well Log Analysts Sixteenth Annual Logging Symposium Transactions, Paper O, New Orleans, Louisiana, June 1975.

Wilson, R.D., and D.C. Stromswold, 1981. *Spectral Gamma-Ray Logging Studies*, GJBX-21(81), prepared by Bendix Field Engineering Corporation for the U.S. Department of Energy Grand Junction Projects Office, Grand Junction, Colorado.